Synthesis of syntactic steel foam using gravity-fed infiltration

G. Castro[1], S.R. Nutt[1]

1. Department of Chemical Engineering and Materials Science, University of Southern California, Los Angeles, CA 90089-0241, USA

Abstract: In this study, we report a procedure for producing syntactic steel foams by melt infiltration of millimeter-sized ceramic microspheres. The gravity-fed infiltration method yields steel foam with uniform distributions of microspheres and negligible unintended porosity. The critical parameters in the manufacturing process are the melt temperature and the preheat temperature of the microspheres prior to infiltration. Syntactic foams with relative density of 0.46 were produced using monosized microspheres (4.45 mm) randomly situated in a mold. Six steel compositions were selected to produce steel foams of different inherent yield strength: five ferritic–pearlitic steels and one TRIP steel (transformation-induced plasticity). The resultant foams were characterized by chemical and microstructural analysis. The microstructure of the samples consisted of blends of ferritic and pearlitic constituents in varying proportions for the ferritic–pearlitic steels, while the cast TRIP steel matrix presented an austenitic microstructure. Simple compression behavior of the steel syntactic foams was studied, and the TRIP steel syntactic foam exhibited the highest compression strength and energy absorption capacity. Syntactic steel foams were also produced with different relative densities (0.60, 0.68 and 0.75). The steel syntactic foam with relative density of 0.60 exhibited the maximum energy absorption. Problems and challenges for achieving steel foams with lower relative densities and for scaling up the synthesis process are contemplated.

Key words: Steel foam; Ceramic microspheres; Melt infiltration; Compression

Please cite this article as G. Castro, S.R. Nutt, **Synthesis of syntactic steel foam using gravity-fed infiltration**, Materials Science and Engineering: A, Volume 553, 15 September 2012, Pages 89-95, ISSN 0921-5093, http://dx.doi.org/10.1016/j.msea.2012.05.097.

1. Introduction

Synthesis of syntactic steel foams presents processing challenges because of the high temperatures involved and the need for applied pressure to promote melt infiltration into ceramic microspheres. Because of this, most efforts to produce syntactic steel foam have relied on powder metallurgy (P/M) techniques [1] and [2]. One such approach involves arranging hollow ceramic/metallic microspheres in a close-packed array, filling interstitial spaces with steel powder, and sintering the assembly to produce syntactic foam [2]. A P/M approach has also been used to produce stochastic steel foams by compacting blends of granular foaming agents and steel powder, then melting the compact to expand the foam [1].

Compared to conventional steel alloys, syntactic steel foams can exhibit a weight reduction of approximate 50% and large increases in impact energy absorption per unit volume and per unit weight [3]. These attributes make syntactic steel foam an attractive candidate for armor applications in military vehicles and improved crashworthiness in civilian vehicles. Furthermore, compared to aluminum foams, steel foams present much higher compression strength, and thus much greater energy absorption per unit volume. Despite density values that exceed those of aluminum foams, they exhibit much higher energy absorption per unit mass. Thus, deploying syntactic steel foam in energy absorber applications would produce space and weight savings in vehicles. Moreover, vehicle systems are largely steel-based, and steel foam affords compatibility with steel components such as chassis and frames.

We describe a method to produce syntactic steel foam using a pressure-less melt infiltration approach. In previous work, pressure was applied to achieve melt infiltration of ceramic

Please cite this article as G. Castro, S.R. Nutt, **Synthesis of syntactic steel foam using gravity-fed infiltration**, Materials Science and Engineering: A, Volume 553, 15 September 2012, Pages 89-95, ISSN 0921-5093, http://dx.doi.org/10.1016/j.msea.2012.05.097.

microspheres [3]. However, in the work described here, the only pressure during melt infiltration is the metallostatic weight of the molten steel. The method offers the advantages of simplicity (no vacuum, gas pressure, centrifugal force or stir casting) and the use of low-cost materials (low-carbon steel and alumina microspheres). Hollow alumina microspheres are used because of the inherent high-temperature stability and high strength. A customized induction furnace was designed for melting small amounts of steel (less than 1 kg) in a crucible. The temperature of the melt is not easily measured, and using a common immersion pyrometer was not possible because of the small crucible (ID = 38.1 mm). Nevertheless, the lab-scale setup was suitable for melting steel to reliably produce syntactic steel foams [1].

2. Experimental

2.1 Materials

Syntactic steel foams were produced from two primary constituent materials – low carbon steel (AISI 1018) and hollow alumina microspheres (Washington Mills Company). Five ferritic–pearlitic steel compositions were obtained by adding specific amounts of carbon and ferrosilicon, as shown in Table 1, yielding foams with different degrees of intrinsic strength and ductility. The five different compositions were chosen to cover a range of steel matrices ranging from ferritic steel (high ductility-low strength) to pearlitic steel (high strength-low ductility). A sixth foam was produced from a high-alloy TRIP-steel (chemical composition 0.03% C, 15.5% Cr, 6.1% Mn, 6.1% Ni, 0.9% Si and 0.1% Al) [4]. The chemical composition was obtained by adding specific amounts of electrolytic iron, carbon, ferrochromium, ferromanganese, nickel, ferrosilicon and aluminum.

Please cite this article as G. Castro, S.R. Nutt, **Synthesis of syntactic steel foam using gravity-fed infiltration**, Materials Science and Engineering: A, Volume 553, 15 September 2012, Pages 89-95, ISSN 0921-5093, http://dx.doi.org/10.1016/j.msea.2012.05.097.

Table 1. *Chemical composition of the ferritic–pearlitic steels.*

Sample	% C	% Si
A	0.20	0.10
B	0.26	0.40
C	0.32	0.70
D	0.38	1.00
E	0.44	1.30

The microspheres were sorted and classified according to size. Mono-sized alumina microspheres with diameters of 4.45 ± 0.15 mm were used for the infiltration experiments. Larger microspheres (4.45 mm diameter – average value) was selected to minimize the resistance to melt infiltration. Smaller microspheres offered greater resistance to infiltration. The microspheres were approximately spherical and showed a slight surface texture. The chemical composition of the alumina microspheres is shown in Table 2.

Table 2. *Chemical analysis of alumina microspheres.*

Component	Percentage
Al_2O_3 (by difference)	99.2
SiO_2	0.60
Fe_2O_3	0.02
Na_2O	0.15
CaO	0.01
Other oxides	0.02

2.2 Foam production

Steel charges were melted using a customized induction furnace (12.5 kW, 10–50 kHz), and a custom-designed crucible was used for the gravity-fed infiltration procedure (Fig. 1). The crucible consisted of two chambers: an upper chamber for melting the steel charge, and a lower chamber (mold) for packing and infiltrating the alumina microspheres. After melting the steel charge in the

Please cite this article as G. Castro, S.R. Nutt, **Synthesis of syntactic steel foam using gravity-fed infiltration**, Materials Science and Engineering: A, Volume 553, 15 September 2012, Pages 89-95, ISSN 0921-5093, http://dx.doi.org/10.1016/j.msea.2012.05.097.

upper chamber (Fig. 1a), the melt flows through an opening in the bottom of the crucible, passes through a ceramic filter, then enters the mold, infiltrating the packed microspheres from bottom to top. Vents were machined in the mold to accommodate displaced gas during melt infiltration, avoiding entrapment of air in the cast sample. During the melt and infiltration process, the duration of each step was controlled to produce repeatable and consistent samples, and experiments were carried out to determine how process variables influenced foam quality.

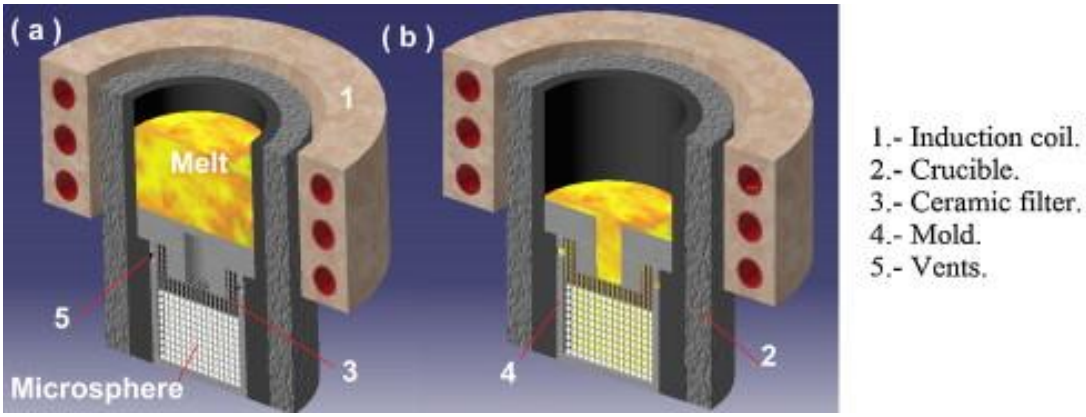

Fig. 1. *Gravity-fed infiltration process.*

2.3 Density

Syntactic foam samples were sectioned to final dimensions of Ø 23 mm × 23 mm (Fig. 2). The density of the syntactic foam was determined by measuring the weight and dimensions of the sample. Thus, the density of the syntactic steel foam sample was 4220 kg/m^3, and the relative density of the steel syntactic foam sample was 0.46 (steel density = 7800 kg/m^3). Image analysis of polished sections revealed that the syntactic steel foam consisted of 63% alumina microspheres and 37% steel matrix by volume. The difference between the relative density (46%) and the steel matrix volume fraction (37%) arose from the weight of the hollow microspheres included in the syntactic foam density. A random collection of mono-sized spheres can be expected to yield a minimum packing

Please cite this article as G. Castro, S.R. Nutt, **Synthesis of syntactic steel foam using gravity-fed infiltration**, Materials Science and Engineering: A, Volume 553, 15 September 2012, Pages 89-95, ISSN 0921-5093, http://dx.doi.org/10.1016/j.msea.2012.05.097.

density of 52.36% [5] and a maximum of 74% when ordered in a close-packed array. A volume fraction of 0.63 corresponds roughly to random dense packing of mono-sized microspheres [5].

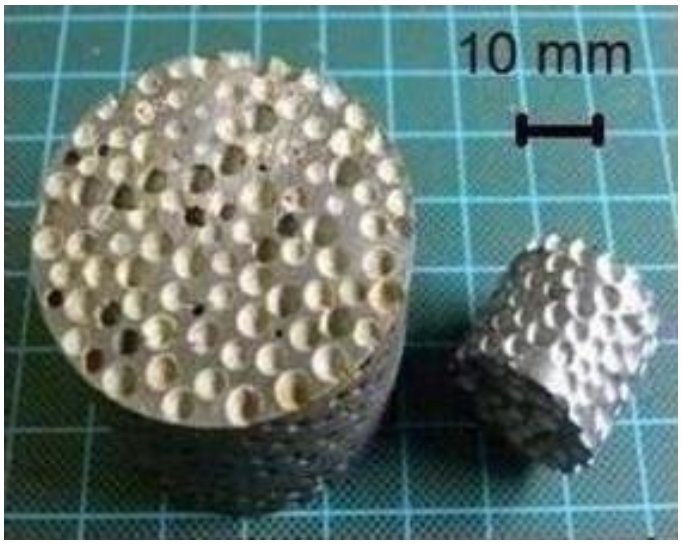

Fig. 2. *Samples of steel syntactic foam produced by gravity-fed infiltration.*

2.4 Microstructure

Polished sections of cast syntactic foam samples were prepared to determine the distribution of microspheres and the quality of the infiltration (Fig. 3). A typical distribution of microspheres in the steel matrix is shown in Fig. 2. After initial infiltration trials, samples were sectioned and examined microscopically to detect unintended porosity (unfilled regions between the microspheres). No unintended porosity or microsphere clustering was observed. Furthermore, there was no sign of broken or cracked microspheres infiltrated with steel in interior regions. Despite mutual contact between adjacent microspheres, melt infiltration occurred at the contact points, and infiltration gaps were not observed.

Please cite this article as G. Castro, S.R. Nutt, **Synthesis of syntactic steel foam using gravity-fed infiltration**, Materials Science and Engineering: A, Volume 553, 15 September 2012, Pages 89-95, ISSN 0921-5093, http://dx.doi.org/10.1016/j.msea.2012.05.097.

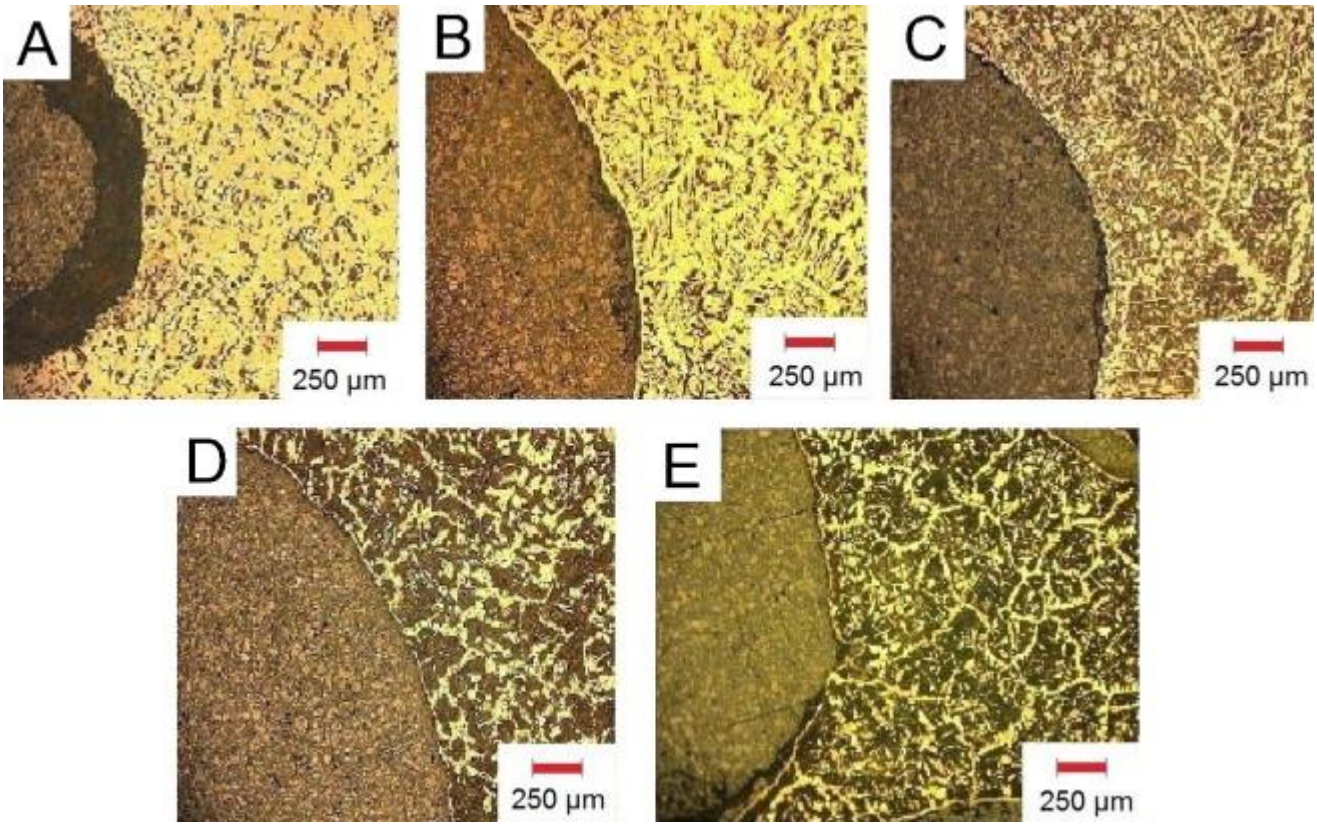

Fig. 3. *Microstructure of the steel syntactic foam samples (A–E).*

2.4 Compression

Compression tests were conducted at a strain rate of 1 mm/min using specimens with dimensions Ø 22.9 mm × 22.9 mm. Three samples for each composition were prepared by polishing prior to testing, and all foam samples tested had a relative density of 0.46 ± 0.1. The compression tests were performed using a load frame (Instron 5585H) and load-displacement data were converted to stress–strain data. The specimen size ensured that each sample tested contained at least six microspheres in each direction, thus minimizing edge effects [6]. Compression tests were conducted at a strain rate of 1 mm/min using specimens with dimensions Ø 22.9 mm × 22.9 mm. Three samples for each composition were prepared by polishing prior to testing, and all foam samples tested had a relative

Please cite this article as G. Castro, S.R. Nutt, **Synthesis of syntactic steel foam using gravity-fed infiltration**, Materials Science and Engineering: A, Volume 553, 15 September 2012, Pages 89-95, ISSN 0921-5093, http://dx.doi.org/10.1016/j.msea.2012.05.097.

density of 0.46 ± 0.1. The compression tests were performed using a load frame (Instron 5585H) and load-displacement data were converted to stress–strain data. The specimen size ensured that each sample tested contained at least six microspheres in each direction, thus minimizing edge effects [6].

3. Results and Discussion

3.1 Microsphere preheatment

For complete infiltration of the microspheres, the melt must remain liquid and fluid during the entire infiltration process. To achieve this, sources of heat loss in the crucible must be minimized or eliminated. The heat loss occurs from pouring the steel melt and from the microspheres exposed at the top of the crucible. For this reason, the crucible and the mold were joined in one assembly and the assembly was heated by induction furnace alone. This method was used to preheat the microspheres to 1100 °C prior to infiltration. The melt flow into the mold was gravity fed and occurred without applied pressure, resulting in complete infiltration. Mold vents allowed for gas escape during the infiltration, eliminating gas entrapment in the cast samples. The most important parameters controlling the infiltration were the preheatment temperature of the microspheres and the melt temperature prior to infiltration.

3.2 Mechanical properties

Quasistatic compression tests were conducted on foam samples at a strain rate of 1 mm/min. The stress–strain curves of samples A, B, C and D exhibit elastic-plastic stress–strain behavior

Please cite this article as G. Castro, S.R. Nutt, **Synthesis of syntactic steel foam using gravity-fed infiltration**, Materials Science and Engineering: A, Volume 553, 15 September 2012, Pages 89-95, ISSN 0921-5093, http://dx.doi.org/10.1016/j.msea.2012.05.097.

characteristic of foams and other cellular materials (Fig. 4a and b). The first stage consists of a linear elastic region, which is followed by a distinct knee characterized by a small positive slope. The stress at this knee is taken as the compression strength for the syntactic foam. The knee is followed by a long hill plateau, during which the cell walls bend, buckle and collapse. Finally, the plateau ends and the stress begins to rise sharply, as the microspheres are completely collapsed and the densification stage begins.

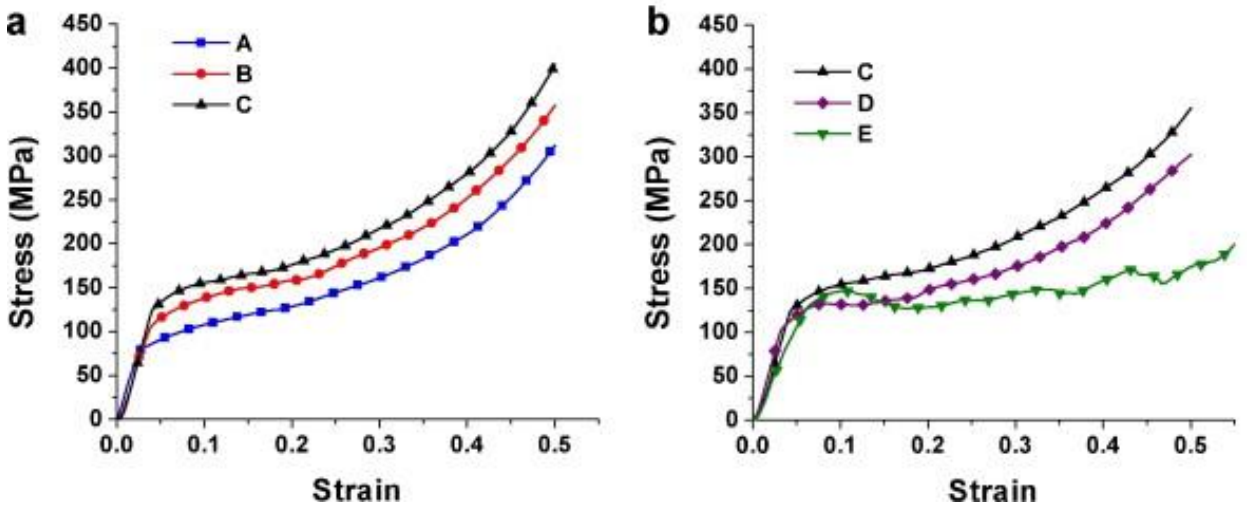

Fig. 4. *Stress–strain curves for steel foams of different C content. (a) Samples A, B and C. (b) Samples C, D and E.*

Fig. 4a (samples A, B and C) shows that the compression strength increases as the alloy content increases (compositions A through C). Increasing the alloy content increases the yield strength of the steel, and thus the foam strength. Note that the slope in this region gradually increases as the deformation progresses and is not perfectly flat (plastic), as in an ideal energy absorber. Normally, strain hardening in stochastic metallic foams is insignificant, but the strain hardening that occurs during the compression of samples A, B and C could be the combined result of the steel matrix ductility and the uniform structure of the steel syntactic foam. In samples D and E, cell walls

Please cite this article as G. Castro, S.R. Nutt, **Synthesis of syntactic steel foam using gravity-fed infiltration**, Materials Science and Engineering: A, Volume 553, 15 September 2012, Pages 89-95, ISSN 0921-5093, http://dx.doi.org/10.1016/j.msea.2012.05.097.

developed cracks as they bent, buckled and collapsed, and as a result, the plateau stress did not increase with increasing strain especially in sample E (Fig. 4b). When cracking occurred in the cell walls, the relationship between the alloy content and the compression strength changed.

Unstable crack propagation causes brittle fragmentation of cell walls (as opposed to plastic bending) and is considered undesirable for the energy absorption function of metallic foams [1]. Fragmentation occurs when the foam material lacks sufficient fracture toughness (K_{IC}) to plastically arrest cracks nucleated on the tension side of bending struts [7]. To resist strut fragmentation failure, the size of the plastic zone ahead of an opening crack tip must be comparable to the strut width. The plastic zone size, K_{IC}^2/σ_y^2, is employed as a characteristic length scale to quantify the material resistance to fracture. For example it is known that cast gray iron has a low value of fracture toughness, therefore steel foams with high carbon contents (2–3% C: gray iron matrix) normally presented serrated stress–strain curves with large stress drops in the stress plateau caused by strut cracking [1]. If struts undergo plastic yielding during collapse (as opposed to fragmentation), the foam will exhibit a higher plateau stress and a higher amount of absorbed energy for a given architecture, metal matrix and relative density [7].

During compression of foam samples, the work done is irreversibly absorbed as plastic deformation. The energy absorbed per unit volume is given by the area under the stress–strain curve up to the onset of densification. Table 3 shows that sample C exhibits greater energy absorption than the other compositions: 1.12 times more energy than sample B and 1.26 times more energy than sample D. Sample C exhibited the strongest matrix of foam samples in which cracking did not occur.

Please cite this article as G. Castro, S.R. Nutt, **Synthesis of syntactic steel foam using gravity-fed infiltration**, Materials Science and Engineering: A, Volume 553, 15 September 2012, Pages 89-95, ISSN 0921-5093, http://dx.doi.org/10.1016/j.msea.2012.05.097.

Table 3. *Energy absorption of syntactic steel foam with different compositions*.

	TRIP steel	A	B	C	D	E
Densification strain (%)	50	50	50	50	50	50
Energy absorption per volume at densification (MJ/m^3)	138.30	78.98	94.02	104.78	85.50	67.82
Energy absorption per mass at densification (kJ/kg)	38.55	22.01	26.20	29.20	23.83	18.90

Insight into deformation mechanisms was provided by images recorded at progressively larger strains, as shown in Fig. 5 and Fig. 6. Sample B deformed smoothly (without fragmentation) up to 50% strain. Cell walls buckled continuously, and collapsing cells were uniformly distributed through the sample during compression. Uniform (non-localized) deformation is reportedly enhanced by foam homogeneity, while heterogeneous foam structures promote deformation bands [8]. After the cell collapse mechanism was exhausted and the ceramic microspheres were completely crushed, some pulverized fragments exfoliated from the sample periphery. Deformation of sample E (Fig. 6) resulted in the development of cracks and associated fragmentation. Such macroscopic cracks have been attributed to the collapse of weak struts and the subsequent formation of deformation bands (manifest as stress oscillations in the stress–strain curve) [8]. Deformation bands reduce compressive strength and compromise the ability to absorb energy. Total fragmentation behavior was not observed in any of the syntactic steel foams produced here – the foams remained intact and in one piece after compression loading.

Please cite this article as G. Castro, S.R. Nutt, **Synthesis of syntactic steel foam using gravity-fed infiltration**, Materials Science and Engineering: A, Volume 553, 15 September 2012, Pages 89-95, ISSN 0921-5093, http://dx.doi.org/10.1016/j.msea.2012.05.097.

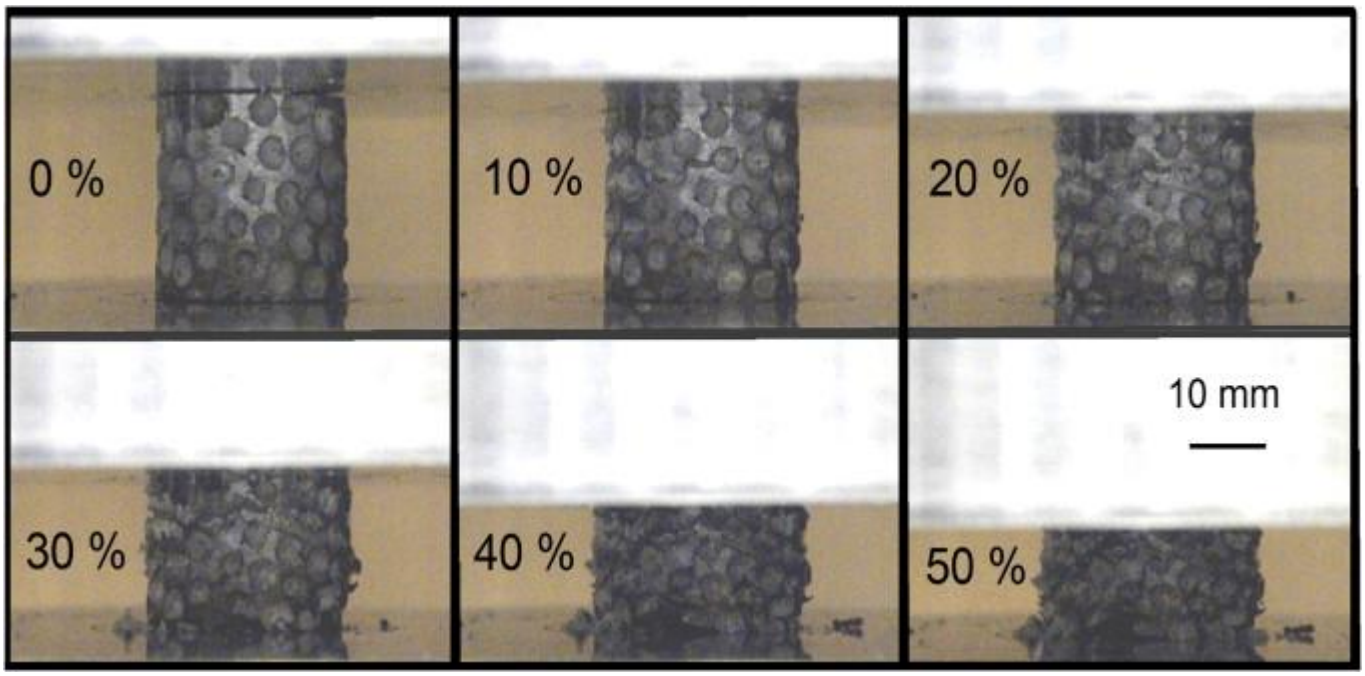

Fig. 5. *Compression of sample B: showing different stages of compression: 0%, 10%, 20%, 30%, 40% and 50% strain.*

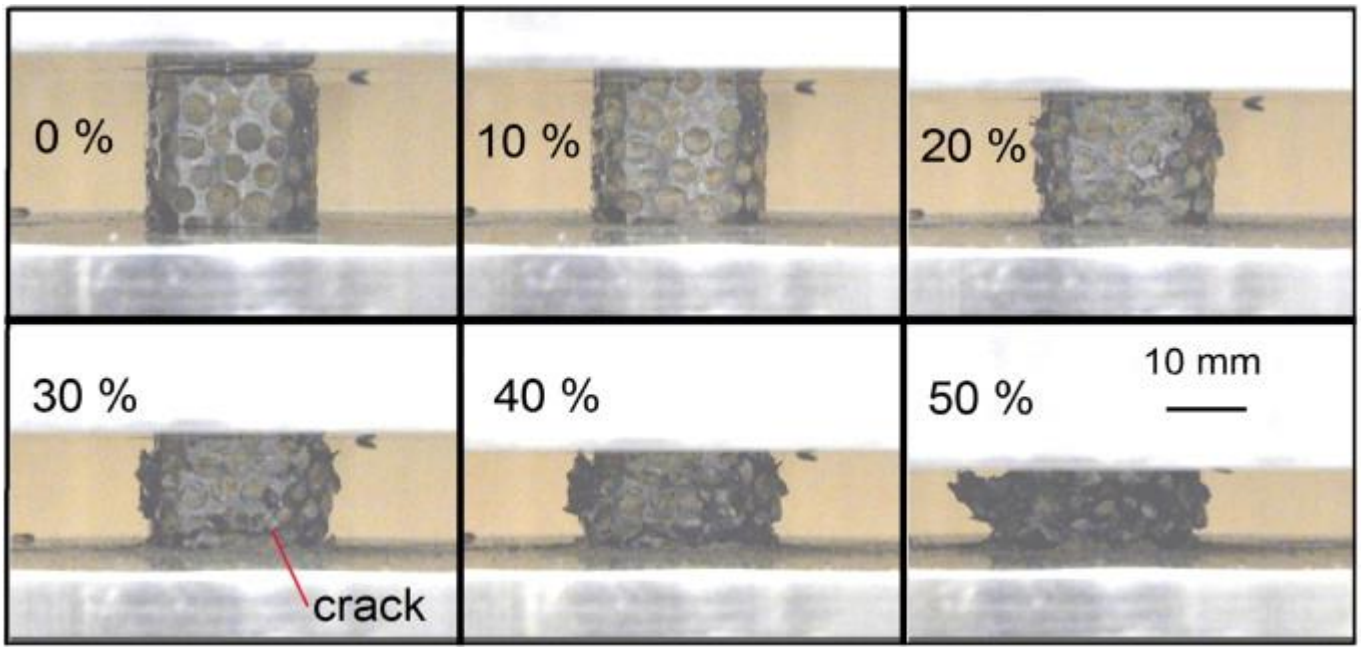

Fig. 6*. Compression of sample E: showing different stages of compression: 0%, 10%, 20%, 30%, 40% and 50% strain.*

Please cite this article as G. Castro, S.R. Nutt, **Synthesis of syntactic steel foam using gravity-fed infiltration**, Materials Science and Engineering: A, Volume 553, 15 September 2012, Pages 89-95, ISSN 0921-5093, http://dx.doi.org/10.1016/j.msea.2012.05.097.

3.3 TRIP steel syntactic foam

One of the primary objectives of foam design is to increase the energy absorbed per unit weight during compression loading. This can be achieved by increasing the yield strength and toughness of the foam material without compromising foam density or densification strain. To pursue this approach, TRIP steel foams (transformation-induced plasticity) were produced. The TRIP acronym derives from the deformation behavior in which the austenitic matrix transforms to martensite, allowing for increased strength and ductility [9]. A casting composition of TRIP-steel was selected (CrMnNi) as opposed to a wrought alloy composition [10]. Fig. 6 shows the stress–strain curve for the TRIP steel foam in as-cast condition. The TRIP steel foam shows higher compression strength relative to the ferritic–pearlitic foams and absorbs approximately 32% more energy than sample C (Fig. 7).

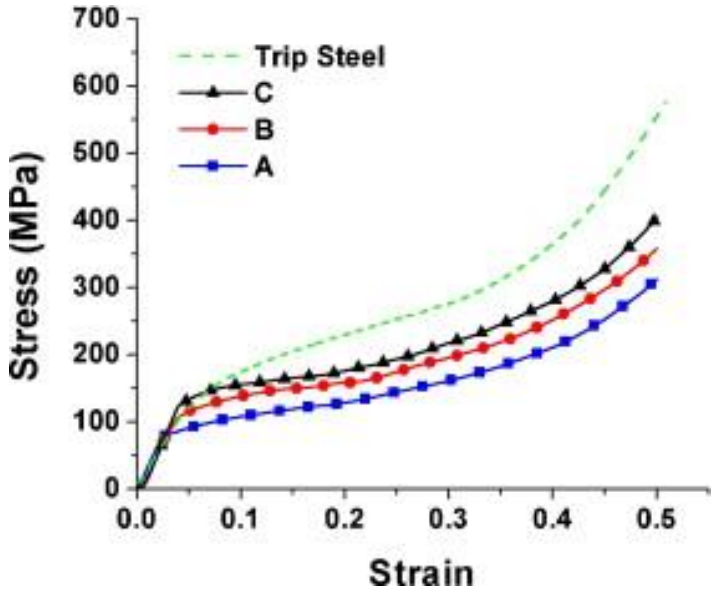

Fig. 7. *Stress–strain curves of samples A, B, C and TRIP steel.*

Please cite this article as G. Castro, S.R. Nutt, **Synthesis of syntactic steel foam using gravity-fed infiltration**, Materials Science and Engineering: A, Volume 553, 15 September 2012, Pages 89-95, ISSN 0921-5093, http://dx.doi.org/10.1016/j.msea.2012.05.097.

3.3 Effect of relative density on mechanical behaviour

Like most foams, the mechanical response of syntactic foams depends most strongly on relative density. While the densification strain can be increased by increasing the microsphere fraction (for example using a bimodal distribution of microspheres) [11], the compression strength will generally decrease. Conversely, reducing the microsphere content generally increases the compression strength, although the densification strain decreases.

The effects of relative density on mechanical behavior were explored by preparing a set of foams with different fractions of microspheres. The primary challenge associated with changing the relative density of syntactic foams is maintaining a uniform distribution of microspheres (without clusters). Mechanical stirring has been used to produce syntactic aluminum foams with variable relative density, but stirring molten steel poses special difficulties, and alternative approaches are required [12]. To ensure uniform dispersions of microspheres, we deployed wire mesh inserts in the microsphere beds to create effective “preforms” for melt infiltration. The mold was filled with alternating layers of wire mesh and packed microspheres, as shown in Fig. 8a. The mesh inserts fixed the microspheres in position, preventing redistribution during melt infiltration. The resultant material was an anisotropic structure of syntactic foam layers alternating with solid steel slabs (from the mesh inserts, Fig. 8b). Wire meshes of different dimensions were used to produce syntactic foams with relative density values of 0.60, 0.68 and 0.75. An alloy composition of 0.32% C, 0.70% Si was used for these foam samples to maximize energy absorption during compression.

Please cite this article as G. Castro, S.R. Nutt, **Synthesis of syntactic steel foam using gravity-fed infiltration**, Materials Science and Engineering: A, Volume 553, 15 September 2012, Pages 89-95, ISSN 0921-5093, http://dx.doi.org/10.1016/j.msea.2012.05.097.

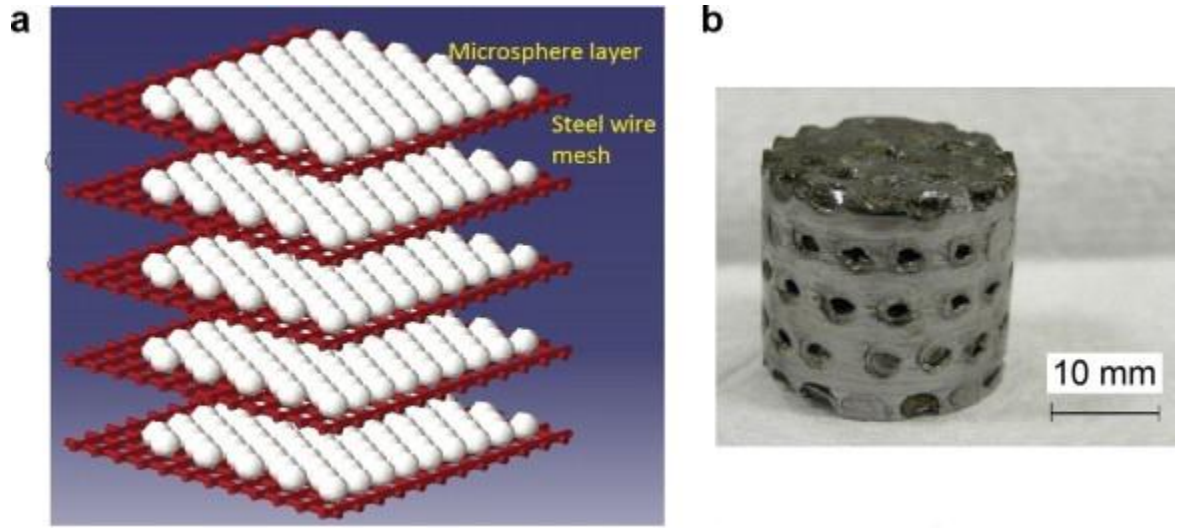

Fig. 8. *(a) Schematics showing the use of wire mesh in the manufacture of syntactic foams. (b) Sample of steel syntactic foam with relative density of 0.60.*

Compression test results for foams of different relative density (RD) are shown in Fig. 9 and include the syntactic foam RD = 0.46 and 1 (fully dense) for comparison purposes. The strain–stress curves show that increasing the relative density of the foam produces an increase in the compression strength and a decrease in the duration of the stress plateau. The sample with relative density of 0.75 absorbs a significant amount of energy per unit volume because of its high compression strength rather than because of a large stress plateau (densification strain of approximately 0.38). Different behavior is shown by the foam of 0.46 relative density that absorbs a good amount of energy but with a lower compression strength and longer plateau duration (densification strain of approximately 0.5).

Please cite this article as G. Castro, S.R. Nutt, **Synthesis of syntactic steel foam using gravity-fed infiltration**, Materials Science and Engineering: A, Volume 553, 15 September 2012, Pages 89-95, ISSN 0921-5093, http://dx.doi.org/10.1016/j.msea.2012.05.097.

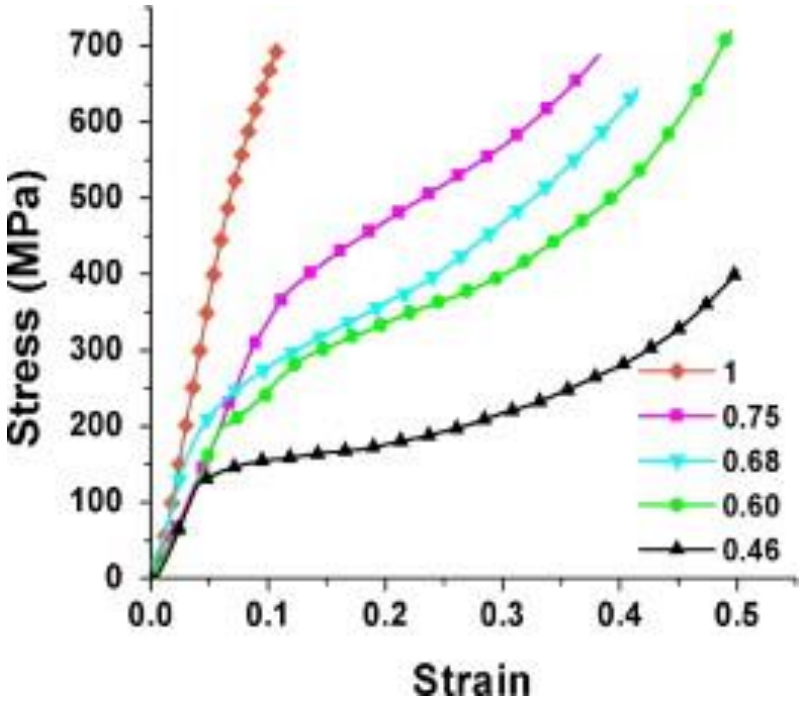

Fig. 9. *(a) Stress–strain curves for steel syntactic foam samples with relative density of 0.46, 0.60, 0.68, 0.75 and 1.*

Table 4 shows the values of energy absorbed per unit volume and per unit weight for the samples with different relative densities. The values in Table 4 were calculated using the densification strain shown in the same table. The densification strain of the steel foam samples was determined from the inflection point in the stress–stress curve (there is no accepted formula or method to determine the onset of densification). Comparing the foams in terms of energy absorbed per unit mass, the syntactic foam with a relative density of 0.6 has the highest energy absorption per unit mass among all the samples.

Please cite this article as G. Castro, S.R. Nutt, **Synthesis of syntactic steel foam using gravity-fed infiltration**, Materials Science and Engineering: A, Volume 553, 15 September 2012, Pages 89-95, ISSN 0921-5093, http://dx.doi.org/10.1016/j.msea.2012.05.097.

Table 4. *Energy absorption of syntactic steel foam with different relative densities and aluminum foam with relative density of 0.148 [13].*

	0.46 RD	0.60 RD	0.68 RD	0.75 RD	1.00 RD	0.148 RD
Energy absorption per volume at densification (MJ/m^3)	104.78	183.23	154.98	161.11	41.27	2.6
Energy absorption per mass at densification (kJ/kg)	29.20	39.15	29.21	27.50	5.29	6.5
Densification strain (%)	0.50	0.49	0.42	0.38	0.11	0.5

The energy absorption capability of a typical aluminum closed-cell foam with relative density of 0.148 [13] is also included in Table 4 for comparison. All of the syntactic steel foams produced in this study have much greater energy absorption capacity than the closed-cell aluminum foam reference material (RD = 0.148). The aluminum stochastic foam absorbs 6.5 kJ/kg (2.6 MJ/m^3) while the syntactic steel foam of 0.6% RD absorbs 39.15 kJ/kg (183.23 MJ/m^3), a six-fold increase. In fact, this particular steel foam absorbs six times more energy per unit of mass, and seventy times more per unit volume compared to the aluminum foam reference material.

The energy absorption capacity of syntactic steel foam also compares favorably to other types of cellular structures, such as egg-box structures and truss core structures. For example, Queheillalt and Wadley [14] reported an average value of 8 kJ/kg (4 MJ/m^3) for hollow lattice truss structures with relative densities ranging from 0.031 to 0.233. These structures consisted of 304 stainless steel solid

Please cite this article as G. Castro, S.R. Nutt, **Synthesis of syntactic steel foam using gravity-fed infiltration**, Materials Science and Engineering: A, Volume 553, 15 September 2012, Pages 89-95, ISSN 0921-5093, http://dx.doi.org/10.1016/j.msea.2012.05.097.

wires and tubes. In other work, Zupan et al. [15] reported a value of 1.44 kJ/kg (0.17 MJ/m^3) for an aluminum egg-box panel with a relative density of 0.044. These values of 8 and 1.44 kJ/kg are far less than the values of 27–39 kJ/kg for steel foams (Fig. 10).

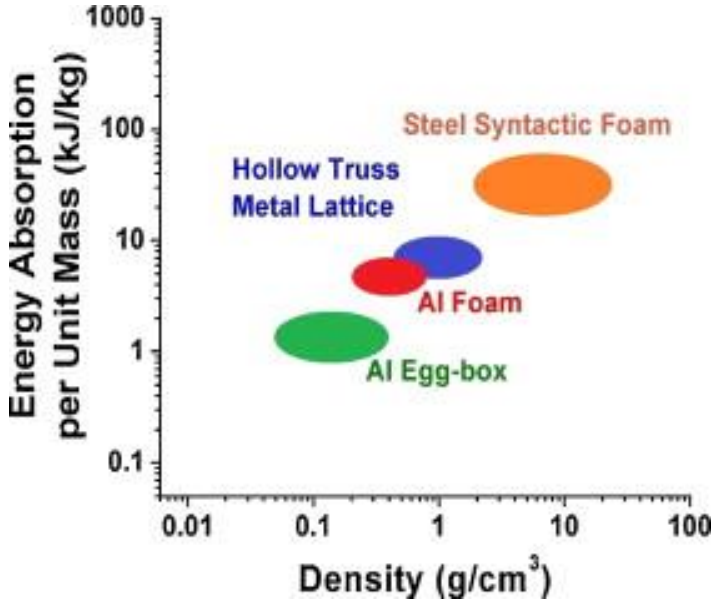

Fig. 10. *Energy absorption per unit mass vs. density: aluminum egg-box [15], aluminum foam [13], hollow truss metallic lattice [14] and 0.6 RD steel syntactic foam.*

To better understand the practical potential of syntactic steel foams, one can calculate the thickness of metallic foam (x) necessary to fully absorb the kinetic energy of a moving vehicle of mass m and velocity v [16]

$$x = \frac{mv^2}{2E_v A} \tag{1}$$

where E_v is the energy absorption per unit of volume and A is the contact area of the metal foam. Assuming an average value of m = 1000 kg, v = 27.78 m/s and A = 0.2 m^2, a piece of aluminum foam 0.74 m thick would absorb all the kinetic energy, while a piece of syntactic steel foam (RD = 0.60)

Please cite this article as G. Castro, S.R. Nutt, **Synthesis of syntactic steel foam using gravity-fed infiltration**, Materials Science and Engineering: A, Volume 553, 15 September 2012, Pages 89-95, ISSN 0921-5093, http://dx.doi.org/10.1016/j.msea.2012.05.097.


would require a thickness of only 0.011 m. Thus, the steel foams produced here are potentially well-suited to applications requiring high impact energy absorption.

The strain–stress curves show that increasing the relative density of the foam increases the compression strength and decreases the duration of the stress plateau. Therefore, by increasing the relative density, the ability to absorb energy at low stress levels decreases. Usually there is a tradeoff between foam strength and densification strain. For example, samples with relative density 0.75 absorb a large amount of energy per unit volume because of the high compression strength rather than the large stress plateau (densification strain of approximately 0.38). Different behavior is exhibited by samples of relative density 0.46, which show lower compression strength but longer plateaus (densification strain of approximately 0.5). The foams absorb similar amounts of energy per unit volume but at different stress levels, thereby expanding the design space for materials selection.

Comparing the energy absorbed per unit mass for the different foams, a syntactic foam with a low compression strength and a long stress plateau can absorb more energy per unit mass than one with a high compression strength and a short stress plateau. Among all the samples produced, the foam with relative density 0.6 showed the greatest energy absorption per unit mass. In practice, foam selection will depend on the application requirements, such as high compression strength and short stress plateau or relatively low compression strength and longer stress plateau.

Please cite this article as G. Castro, S.R. Nutt, **Synthesis of syntactic steel foam using gravity-fed infiltration**, Materials Science and Engineering: A, Volume 553, 15 September 2012, Pages 89-95, ISSN 0921-5093, http://dx.doi.org/10.1016/j.msea.2012.05.097.

4. Conclusions

A method for producing syntactic steel foams by melt infiltration is described and demonstrated with six alloy compositions. A relative density of 0.46 (corresponding to 3.59 g/m^3) was achieved using monosized (4.45 mm diameter) microspheres. The foams showed no unintended porosity or clustering of microspheres. The critical parameters in the manufacturing of the steel syntactic foams were the steel melt temperature and the preheat temperature of the microspheres prior to infiltration.

All of the steel foams produced in this study exhibited elastic-plastic foam behavior in compression – an initial linear elastic region followed by a long hill plateau, culminating in densification. Maximizing the intrinsic strength and toughness of the steel (as in TRIP steel) yielded the foam with the greatest compression strength and energy absorption capacity. Syntactic steel foams with different relative densities were also produced and tested, showing that the foam with RD = 0.60 exhibited the maximum energy absorption. The results demonstrate that maximizing energy absorption capacity requires selecting an optimal relative density range (and microsphere distribution), as well as balancing intrinsic strength and toughness of the foam metal. Note that all of the steel foams surpassed the energy absorption capacity of Al foams, some by as much as a factor of 6 per unit weight and by a factor of 70 per unit volume.

The energy absorption values of the prototype steel foams compare favorably to other energy absorbing cellular structures, such as metallic trusses or egg-box structures. Superior performance is achieved with relatively low-cost constituent materials and a scale-able, low-cost method of manufacture based on gravity-fed casting. The casting method employed here can also be extended to molds with different geometries and to other variants of the casting technique. Potential

Please cite this article as G. Castro, S.R. Nutt, **Synthesis of syntactic steel foam using gravity-fed infiltration**, Materials Science and Engineering: A, Volume 553, 15 September 2012, Pages 89-95, ISSN 0921-5093, http://dx.doi.org/10.1016/j.msea.2012.05.097.

applications of steel syntactic foam are expected to arise in the automotive industry, in the military and in civil defense structures. They can be used as bumpers for railcars, trams and automobiles, in vehicles that requires protection from ballistic impact, and in structures that provide blast protection from explosives.

References:

1. C. Park, S.R. Nutt, Mater. Sci. Eng. A 288 (1) (2000) 111–118.
2. B.P. Neville, A. Rabiei, Mater. Des. 29 (2) (2008) 388–396.
3. G. Castro, S.R. Nutt, Mater. Sci. Eng. A 535 (2012) 274–280.
4. S. Martin, S. Wolf, U. Martin, L. Krüger, A. Jahn, ESOMAT 2009 (2009) 05022, http://dx.doi.org/10.1051/esomat/200905022.
5. A. Rabiei, A.T. O'Neill, Mater. Sci. Eng. A 404 (1–2) (2005) 159–164.
6. Y. Sirong, L. Jiaan, L. Yanru, L. Yaohui, Mater. Sci. Eng. A 457 (1–2) (2007) 325–328.
7. J.P. Schramm, D.C. Hofmann, M.D. Demetriou, W.L. Johnson, Appl. Phys. Lett. 97 (241910) (2010).
8. A. Ohrndorf, U. Krupp, ICF XI – 11th International Conference on Fracture, 2005.
9. M. Weider, K. Eigenfeld, Steel Res. Int. 82 (9) (2011) 1064–1069, http://dx.doi.org/10.1002/srin.201100071.
10. L. Krüger, S. Wolf, U. Martin, S. Martin, P.R. Scheller, A. Jahn, A. Weiß, J. Phys. 240 (2010) 012098.
11. X.F. Tao, L.P. Zhang, Y.Y. Zhao, Mater. Des. 30 (7) (2009) 2732–2736.
12. A. Daoud, Mater. Sci. Eng. A 28 (2008) 1–295.
13. D. Ruan, G. Lu, F.L. Chen, E. Siores, Compos. Struct. 57 (1–4) (2002) 331–336.
14. D.T. Queheillalt, H.N.G. Wadley, Acta Mater. 53 (2) (2005) 303–313.
15. M. Zupan, C. Chen, N.A. Fleck, Int. J. Mech. Sci. 45 (5) (2003) 851–871.
16. E.M.A. Maine, M.F. Ashby, Mater. Des. 23 (2002) 307–319.

Please cite this article as G. Castro, S.R. Nutt, **Synthesis of syntactic steel foam using gravity-fed infiltration**, Materials Science and Engineering: A, Volume 553, 15 September 2012, Pages 89-95, ISSN 0921-5093, http://dx.doi.org/10.1016/j.msea.2012.05.097.